Proc. Natl. Acad. Sci. USA
Vol. 91, pp. 8170–8174, August 1994
Neurobiology

Visualizing hippocampal synaptic function by optical detection of Ca^{2+} entry through the *N*-methyl-D-aspartate channel

(fura-2/facilitation/quantal analysis)

ROBERTO MALINOW*†, NIKOLAI OTMAKHOV*‡§, KENNETH I. BLUM¶‖, AND JOHN LISMAN¶‖

¶Marine Biological Laboratory, Woods Hole, MA 02543; ‖Department of Biology and the Center for Complex Systems, Brandeis University, Waltham, MA 02254; *Department of Physiology and Biophysics, University of Iowa, Iowa City, IA 52242; and ‡Institute of Theoretical and Experimental Biophysics, Russian Academy of Science, Puschino-on-Oka, Russia

Communicated by Philip Siekevitz, April 15, 1994

ABSTRACT **Fura-2 and imaging technology were used to detect intracellular Ca^{2+} changes in CA1 pyramidal cells in hippocampal slices. During focal synaptic stimulation, one or more highly localized regions of Ca^{2+} elevation (hot spots) were detected in the dendrites. Ca^{2+} spread from the center of hot spots with properties consistent with diffusion. Several lines of evidence indicate that these hot spots were due to Ca^{2+} entry through *N*-methyl-D-aspartate synaptic channels. The spatial and temporal resolution of the method was sufficient to detect the response of single hot spots to single stimuli, thus providing a real-time method for monitoring local synaptic activity. Using this method, we show that synapses on the same dendrite differ in their probability of response and in their facilitation properties.**

Long-term potentiation (LTP) in the CA1 region of the hippocampus is triggered by the entry of Ca^{2+} through the *N*-methyl-D-aspartate (NMDA) class of glutamate-activated channels (1, 2). This entry is thought to be localized near active synapses and may thus underlie the synapse specificity of LTP. Several groups have sought to image Ca^{2+} entry through NMDA channels during synaptic stimulation. Initial work detected localized Ca^{2+} signals that could be attenuated by antagonists of the NMDA channel (3–5). However, the origin of these signals remained ambiguous because Ca^{2+} entry through voltage-dependent Ca^{2+} channels is triggered secondarily by the NMDA component of the excitatory postsynaptic potential (EPSP) (6). We therefore attempted to design experiments not subject to this ambiguity. While this work was in progress, two reports using related strategies have appeared (7, 8).

A second goal of our work was to explore the possibility that local Ca^{2+} entry through the NMDA channel could be used as a real-time monitor of synaptic activity. The current methods for studying central synapses are electrical and have the disadvantage that the recorded response is the summation of all active synaptic inputs. Even a single presynaptic axon may make multiple synapses with the same postsynaptic cell (9). Analysis of summed responses is particularly problematic since different synapses may have different properties (10, 11). It is thus desirable to develop an optical indicator of synaptic activity that would allow individual synapses to be monitored. The ultimate goal would be optical quantal analysis of these synapses. Recent work indicates that it is possible to use Ca^{2+} entry through the NMDA receptor to detect single spontaneously released quanta in hippocampal cell cultures (12). The results we present here show that similar signals can be recorded in hippocampal slices during evoked synaptic transmission. This allows optical analysis of transmission in the slice preparation where plasticity (paired-pulse facilitation, LTP, etc.) has been most thoroughly characterized.

The publication costs of this article were defrayed in part by page charge payment. This article must therefore be hereby marked "*advertisement*" in accordance with 18 U.S.C. §1734 solely to indicate this fact.

METHODS

Rat (Long–Evans, 8–14 days old) hippocampal slices (400–500 μm) were prepared by the chopper method using standard procedures (13) and maintained at 22–25°C in an oxygenated/humidified interface incubation chamber for 1 hr. Slices were transferred to a submerged recording chamber and perfused with a solution equilibrated with 95% O_2/5% CO_2, maintained at 22–25°C, containing (in mM) NaCl, 119; KCl, 2.5; $MgCl_2$, 1.3; $CaCl_2$, 2.5; $NaHCO_3$, 26.2; and glucose, 11 (pH 7.4).

Whole cell recordings (Axopatch 1D; Axon Instruments, Burlingame, CA) were obtained under visual control (Zeiss 40× water immersion objective) with pipettes (1–3 MΩ) containing (in mM) cesium gluconate, 100; EGTA, 0.2; $MgCl_2$, 5; ATP, 2; GTP, 0.3; Hepes, 40 (pH 7.2 with CsOH); and reduced glutathione, 5, and adjusted to 300 mosM with sucrose. After allowing 5–10 min for the fura-2 to diffuse into the cell, the neuron was depolarized to −15 mV, illuminated by epifluorescence, and visualized using an air-cooled charge-coupled device camera (Photometrics, Tucson, AZ) under computer control (14). Depolarization initially caused a large increase in Ca^{2+}, which eventually declined to a level in which dendritic fluorescence, F (see definition below), was >50% of the resting level. The current required for maintained depolarization was small (0–20 pA) because of block of potassium channels by Cs^{2+}.

The filled neuron was positioned with a movable stage to reveal a dendritic region of interest (generally ≈100–300 μm from the cell body). The tip of a glass stimulating electrode (1–3 MΩ) containing perfusate solution was marked with an insoluble fluorescent dye and positioned under visual control. Synaptic transmission was elicited by passing 1- to 5-μA, 100-μs pulses. Total fluorescence (f, in arbitrary intensity units) was corrected for baseline drift and for autofluorescence to allow computation of dendritic fluorescence F, the change ΔF, and the ratio $\Delta F/F$. Autofluorescence was measured at a position near the filled dendrite, but there is considerable ambiguity in the determination of the proper value because of the scatter of light from regions of the dendrite that are inactive. The values of $\Delta F/F$ should therefore be considered approximate and could be in error in cases where the autofluorescence correction was large. This ratio

Abbreviations: NMDA, *N*-methyl-D-aspartate; LTP, long-term potentiation; EPSP, excitatory postsynaptic potential; APV, DL-2-amino-5-phosphonovaleric acid.

†To whom reprint requests should be sent at the present address: Cold Spring Harbor Laboratory, P.O. Box 100, Cold Spring Harbor, NY 11724.

§Present address: Department of Biology, Brandeis University, Waltham, MA 02254.

is approximately proportional to the change in intracellular Ca^{2+} concentration until dye saturation occurs at ≈0.8. Generally the values of $\Delta F/F$ were considerably below this value (see figures). All measurements were made at a single excitation wavelength (380 nm). Emission was measured at wavelengths longer than 500 nm. Data were typically collected continuously at 100 ms per frame and digitally filtered where necessary.

RESULTS

To investigate Ca^{2+} entry through synaptic NMDA channels, we obtained whole cell recordings from CA1 pyramidal cells in hippocampal slices. The membrane potential was continuously depolarized to −15 mV to relieve the Mg^{2+} block of the NMDA channel (15, 16) and thereby maximize Ca^{2+} entry when NMDA channels were activated by transmitter release. To detect Ca^{2+} elevations, the Ca^{2+} indicator fura-2 (17) was delivered through the recording pipette. A relatively high concentration (0.7–2 mM) of dye was used, with the goal of obtaining a signal proportional to Ca^{2+} flux (18). A stimulating electrode was positioned 20–40 μm from a dendrite of interest. Trains of stimulating pulses were given and the optical signals were analyzed on-line for hot spots of Ca^{2+} elevation. Stimulus current was increased until an optical signal was detected. Under these conditions, stimulation evoked small (<100 pA; typically ≈10 pA) synaptic currents and one or more hot spots of Ca^{2+} elevation in the nearby dendritic region (n = 24). Fig. 1 *A* and *C* show such a hot spot at 0.9 s after the onset of a stimulation. In this and all subsequent figures, the signals are presented in terms of the fractional change in dendritic fluorescence ($\Delta F/F$), a quantity that reflects the *change* in Ca^{2+} (see *Methods*).

The time course of Ca^{2+} at the center of the hot spot and at nearby locations is shown in Fig. 1*B*. In the central region, Ca^{2+} rose for the entire period of the electrical response and then immediately started to fall (Fig. 1*B*). In flanking regions, the Ca^{2+} elevation appeared to be due to diffusion of Ca^{2+} from the central region: the Ca^{2+} rise was smaller and was delayed relative to the central region. Furthermore, Ca^{2+} continued to rise in flanking regions when the Ca^{2+} level in the central region was falling. This is shown in Fig. 1*D*, which is a pseudocolor presentation of the change in Ca^{2+} during a period between 0.8 and 1.8 s after the stimulus. During this period, Ca^{2+} rose in two flanking regions, whereas it fell in the center of the hot spot (decreases show up as black in Fig. 1*D*). It thus appears that Ca^{2+} spreads within seconds over a region of about 10 μm. This is very similar to the spread of Ca^{2+} entry that occurs during a spontaneous quanta (12).

We sought to determine whether hot spots were generated by Ca^{2+} entry through NMDA channels or through voltage-dependent Ca^{2+} channels. This second possibility needs to be considered because voltage control in the dendrites cannot be ensured during rapid synaptic events (19). Synaptic depolarization produced by current through the NMDA channels may therefore produce Ca^{2+} entry by activation of voltage-dependent Ca^{2+} channels (6). To distinguish between these possibilities, we voltage-clamped the membrane to a voltage sufficiently positive (+20 mV) to reverse the synaptic current evoked by a brief burst (Fig. 2 *A* and *B*). The perfusate contained 100 μM picrotoxin to ensure that the reversal

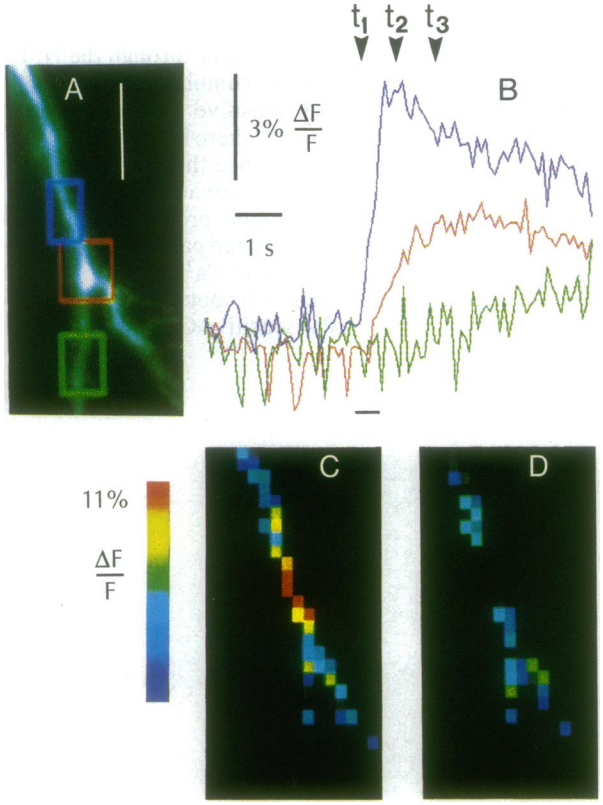

FIG. 1. Spatial and temporal changes of Ca^{2+} at a hot spot caused by burst of synaptic stimulation (10 shocks at 20 Hz, bar). (*A*) Fluorescent image of fura-2 filled cell. Calibration bar = 15 μm. (*B*) Time course of the Ca^{2+} change ($\Delta F/F$) at the regions marked by boxes in *A*. Ca^{2+} in the flanking region rises while Ca^{2+} in the center falls, suggesting diffusion. (*C*) Pseudocolor picture of change in signal during early parts of the response ($t_2 - t_1$ = 0.8 s; t_1 = stimulus onset). (*D*) Change in signal during late parts of the response ($t_3 - t_2$; t_3 = 1.7 s). A symmetrical rise occurs in flanking regions while Ca^{2+} falls in the center of the hot spot (decreases are black). f = 181; autofluorescence = 74.

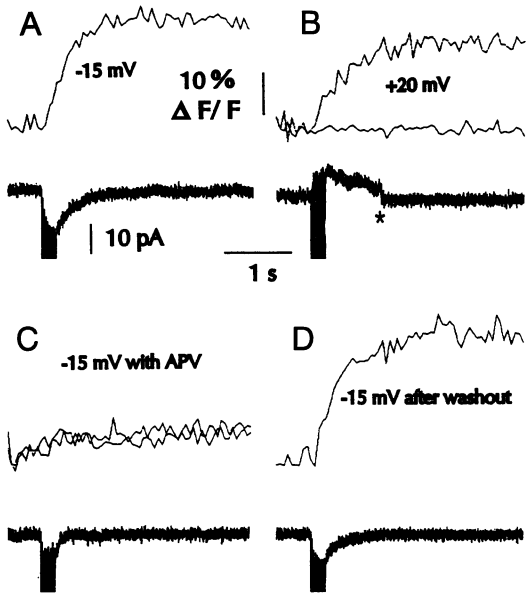

FIG. 2. Local optical signals are due to Ca^{2+} entry through the NMDA channel. (*A*) Synaptically activated Ca^{2+} elevation (top) and inward current (below) produced by a train of 10 stimuli at 50 Hz (vertical deflections) at a holding voltage of −15 mV. (*B*) Synaptically activated Ca^{2+} elevation is evident at +20 mV, which reverses the excitatory synaptic current (asterisk marks electrometer autozero artifact). Baseline is included to show that the nearby dendritic region is inactive. (*C*) In the presence of 50 μM DL-2-amino-5-phosphonovaleric acid (APV), the calcium signal and a slowly decaying component of the synaptic current are blocked. Two traces are superposed to emphasize that the lack of response is unlikely to be due to statistical transmission failure (see Figs. 3 and 4). No failures were observed without APV. (*D*) Washout of APV restores signals. All measurements are from the same cell.

potential of the synaptic current was determined solely by the excitatory conductances. If the clamp were to fail under conditions where the excitatory current was reversed, the membrane potential would hyperpolarize, close voltage-dependent Ca^{2+} channels, and reduce Ca^{2+} entry. What was observed, however, was a synaptically stimulated rise in Ca^{2+} (Fig. 2*B*; $n = 4$). This is consistent with Ca^{2+} entry through the NMDA channels; it is known from previous work that inward Ca^{2+} flux can occur through these channels even under conditions where the net cation flux is outward (20).

As a further test, we applied APV, a competitive NMDA receptor antagonist. APV dramatically reduced the Ca^{2+} signal ($n = 3$) in a reversible fashion (Fig. 2 *C* and *D*). This signal was a local signal, as evidenced by absence of signal in a nearby (50 μm) region of the dendrite (Fig. 2*B*; lower optical trace). The Ca^{2+} signal in APV was undetectable, but values <20% of control cannot be excluded because of background noise. The signal could also be reduced by hyperpolarizing the cell (not shown), as expected given the voltage-dependent block of the NMDA channel by Mg^{2+} (15, 16). We conclude that local synaptically induced Ca^{2+} entry is primarily a consequence of Ca^{2+} entry through the NMDA channel.

The optical signals could be evoked by trains of pulses (Figs. 1 and 2) as previously shown (4–8, 21); however Fig. 3 *A* and *B* show that even single shocks could evoke a detectable response. Fig. 3*B* shows the amplitude histogram of responses evoked by single shocks (light line) and the amplitude histogram of the baseline in the absence of stimulation (dark line). Comparison of the histograms (normalized to equal area) shows that the evoked responses are larger than expected from baseline noise. The responses were clearly larger than the background noise in at least half the trials, indicating that the probability of response at this hot spot was >0.5. There was no clear correspondence of the optical signals with simultaneous electrical signals (not shown), probably because of the involvement of synapses on other dendritic branches.

In other experiments we observed hot spots with a much lower probability of response. Fig. 3*C* shows a hot spot where even trains of 10 stimuli sometimes failed to evoke a response. In cases where trains did evoke a response (third and fifth traces), there were multiple failures of response to shocks before the response occurred. Results such as these indicate that the probability of a response (per stimulus) at some hot spots can be much lower than 0.5 (see also Fig. 4).

Previous work using electrical recording has shown that hippocampal synapses facilitate during high-frequency stimulation (22). Fig. 4 shows a hot spot (site B) where facilitation could be detected optically. The same number of stimuli were delivered in trains at low (2 Hz) and high (20 Hz) frequency. No response was observed at low frequency, but a response was observed at high frequency (Fig. 4*B*). Multiple presentations of trains at these two frequencies showed a consistent difference (Fig. 4*C*). Surprisingly, a second hot spot (site A) on the same dendrite showed almost no facilitation. In general, we found that sites were heterogenous in their facilitation properties; many sites showed considerable facilitation while others showed relatively little. In 9 of 16 hot spots, the average response at low (0.5–5 Hz) frequency was statistically indistinguishable from the average at high frequency (10–50 Hz), as shown in Fig. 4*D Lower*. At these hot spots, $(\Delta F/F)_{\text{low freq}}/(\Delta F/F)_{\text{high freq}} = 1.32 \pm 0.35$. In 7 of 16 hot spots, there was a statistically significant difference between the response to high and low frequency (Fig. 4*D Upper*). In this group, $(\Delta F/F)_{\text{low freq}}/(\Delta F/F)_{\text{high freq}} = 0.2 \pm 0.09$. Of these 7 hot spots, there were 3 in which low-frequency stimulation never produced a response, but high-frequency stimulus consistently did (e.g., site B). These sites were silent during low-frequency stimulation and could only be detected using high-frequency stimulation.

DISCUSSION

The first direct evidence that Ca^{2+} entry through the NMDA channel contributes to synaptically stimulated Ca^{2+} elevation was the detection of an APV-sensitive component of this elevation (4, 5, 7, 8, 21). However, there is some uncertainty about the origin of these signals since they could be due to voltage-dependent Ca^{2+} channels activated as a secondary result of the synaptic depolarization produced by NMDA channels (6). Our work, and two related papers (7, 8), provide evidence that there is a component of Ca^{2+} entry through the NMDA channel that gives rise to hot spots of Ca^{2+} elevation. These experiments show APV-sensitive Ca^{2+} elevations that

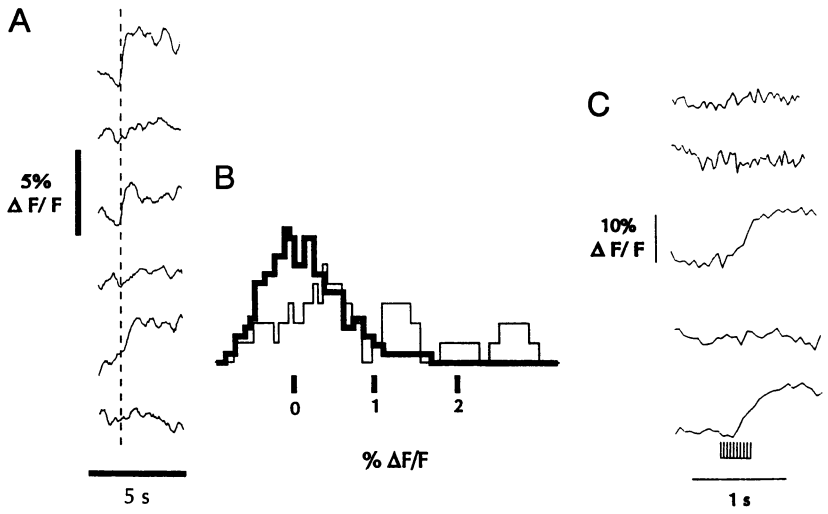

FIG. 3. Heterogeneity of the probability of response. (*A*) At this hot spot, single shocks (given at dashed line) often produced a response (successive traces). Voltage = −15 mV. Shocks were delivered once every 3 min (responses were analyzed on-line). Optical traces were digitally filtered at 1 Hz. $f = 58$; autofluorescence = 40. (*B*) Rolling window estimator of probability density of optical signal measured after stimulation (thin line) and without stimulation (thick line). Responses were calculated by subtracting the signal 0.3 s after the stimulus from the average signal during the last 0.3 s before the stimulus. A rolling histogram was then formed by finding the number of responses that fell within a window that was ±0.25% for each value of $\Delta F/F$. Histograms were then normalized for equal area. (*C*) Different hot spot with much lower probability of response. Successive responses to trains of 10 shocks (20 Hz) delivered every 3 min are shown. Some trains produce no response, indicating that the probability of response to single shocks must be very low. $f = 58$; autofluorescence = 40.

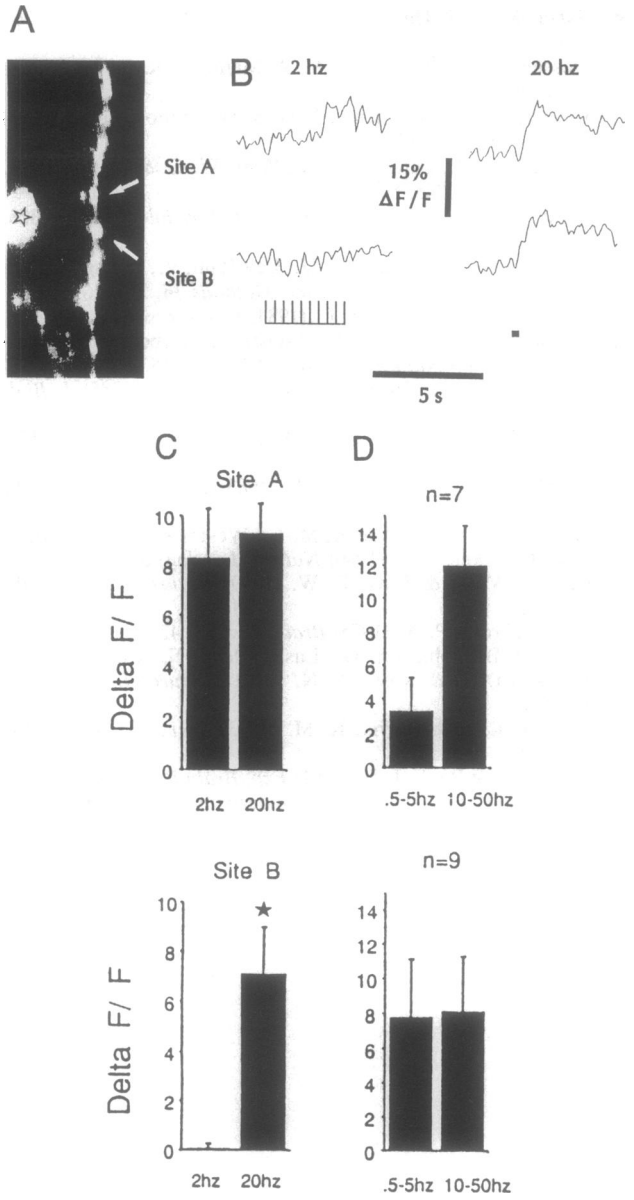

FIG. 4. Frequency facilitation is heterogeneous. (*A*) Fluorescent image of filled dendrite with two hot spots (8 μm apart) exhibiting different degrees of facilitation. The stimulating electrode tip (out of focus) is indicated by the star. (*B*) Examples of responses to 10 stimuli delivered at 2 Hz and 20 Hz at sites A and B. f = 89; autofluorescence = 64. (*C*) Summary data (mean ± SE) for peak response to 2-Hz (n = 4) and 20-Hz (n = 7) stimulation at sites A and B. Use of peak response during 10 stimuli assumes linear integration of responses to individual stimuli (no decay). Responses to individual stimuli measured showed some decay (<25% in 5 s). However since responses generally occurred in the middle of trains, the error introduced by incomplete integration is small. (*D Lower*) In 9 of 16 hot spots, the average response at low (0.5–5 Hz) frequency was statistically indistinguishable from the average at high frequency (10–50 Hz). The average and SE of responses at these hot spots are shown [$(\Delta F/F)_{\text{low freq}}/(\Delta F/F)_{\text{high freq}} = 1.32 \pm 0.35$]. (*D Upper*) In 7 of 16 hot spots, there was a statistically significant difference between the response to high and low frequency. Average = $(\Delta F/F)_{\text{low freq}}/(\Delta F/F)_{\text{high freq}} = 0.2 \pm 0.09$. In this group there were three cases in which low-frequency stimulation never produced a response, but high-frequency stimulus consistently did (e.g., site B). Voltage = −15 mV.

cannot be attributed to voltage-dependent Ca^{2+} channels either because these channels are "washed out" (7) or because the voltage is so positive that any synaptic potentials should be hyperpolarizing and therefore close Ca^{2+} channels (refs. 7 and 8 and Fig. 2). One possible source of concern about the latter strategy is that synapses very distant from the soma might still cause a local depolarization that could activate Ca^{2+} channels even though the synapses closer to the cell body produced hyperpolarizing synaptic responses. This possibility seems unlikely given our results with the focal stimulation method, which selectively excites synapses near the stimulating electrode.

Given these results and those of others (3–5, 7, 8), the following general picture emerges of how synaptic stimulation changes Ca^{2+} levels. The EPSP triggers a widespread elevation of Ca^{2+} through voltage-dependent Ca^{2+} channels. These channels are opened as a direct result of the EPSP (6) and also by action potentials that invade the dendrites (23). Superposed on this spatially diffuse signal are small hot spots of Ca^{2+} elevation at the sites of active synapses. Most of the signal at hot spots is due to Ca^{2+} entry through the NMDA channel, a signal that may be amplified by Ca^{2+} released from internal stores of Ca^{2+} (7).

Our experiments have used focal stimulation, a procedure that brings the stimulating electrode close to a dendritic region of interest. This procedure has some advantages over typical stimulation procedures that use larger electrodes placed more distantly from the cell. Using focal stimulation we always found active synapses close to the stimulating electrode. This made it relatively easy to search on-line for active synapses using our data analysis program. So few synapses are stimulated and the dendritic tree is so vast that the active synapses would otherwise be very time consuming to find. Once one knows where an active synapse is, one can restrict the area of observation and thus the number of pixels acquired. Under certain circumstances this makes it possible to achieve higher time resolution.

The detection of Ca^{2+} entry through the NMDA receptor provides a powerful method for monitoring synaptic function. The fact that even single shocks can produce a detectable local signal (Fig. 3) suggests that optical quantal analysis may be possible. Indeed, a recent report (12) shows that Ca^{2+} signals due to single spontaneous quanta can be detected in cultured hippocampal neurons. Compared to the available electrical methods, the optical method has the important advantage of allowing analysis of responses generated at anatomically distinct sites. This is of particular importance if synapses onto cells are heterogeneous, as our results and those of others (10, 11, 24) strongly suggest.

We have used the optical method to study the synaptic responses to individual stimulation pulses. One striking finding is that some sites respond to stimulation pulses with low probability, whereas others respond with much higher probability. This variability might reflect differences in the probability of firing the presynaptic axon, in the probability of the action potential reaching the synapse (i.e., propagation failure), or in the probability that an active presynaptic bouton will release transmitter. Distinguishing among these possibilities will require the development of methods for monitoring the occurrence of action potentials in the presynaptic bouton. Using altogether different methodology, two groups have recently reported that some hippocampal synapses have a very low probability of vesicle release, whereas others have a high probability (10, 11). Given these results, it would seem likely that the differences we have observed are indeed due to heterogeneity of release probability.

A second finding of importance is the heterogeneity of facilitation. Some sites showed little or no facilitation while others showed dramatic facilitation. Again, we cannot be certain whether this reflects differences in firing of the axon or in the facilitation properties of transmission itself. In either case, however, these results have important implications for physiological experiments since they show that there is a class of hippocampal synapses that may be virtually silent

during low-frequency stimulation but that are active during high-frequency stimulation. One implication is that synapses may filter out low-frequency action potentials ("noise") yet reliably transmit the high-frequency bursts that can be generated by hippocampal neurons (25, 26). Another implication follows from the fact that low-frequency stimulation is used to induce long-term depression (LTD), whereas high-frequency stimulation is often used to induce LTP. Our results thus imply that some synapses transmit reliably during LTP induction but transmit poorly during LTD induction.

We thank Wade Regehr for comments on the manuscript. This work was supported by National Institute of Neurological Disorders and Stroke Grant NS27337-06 (to J.L.) and National Institute of Mental Health Grant HM49159-04 (to R.M.). K.I.B. was supported by National Institutes of Health Training Grant NS07292.

1. Wigstrom, H., Gustafson, B. & Huang, Y.-Y. (1985) *Acta Physiol. Scand.* **123,** 519–521.
2. Bliss, T. V. P. & Collingridge, G. L. (1993) *Nature (London)* **361,** 31–39.
3. Regehr, W. G., Connor, J. A. & Tank, D. W. (1989) *Nature (London)* **341,** 533–536.
4. Muller, W. & Connor, J. A. (1991) *Nature (London)* **354,** 73–76.
5. Regehr, W. G. & Tank, D. W. (1992) *J. Neurosci.* **12,** 4202–4223.
6. Miyakawa, H., Ross, W. N., Jaffe, D., Callaway, J. C., Lasser-Ross, N., Lisman, J. E. & Johnston, D. (1992) *Neuron* **9,** 1163–1173.
7. Alford, S., Frenguelli, B. G., Schofield, J. G. & Collingridge, G. L. (1993) *J. Physiol. (London)* **469,** 693–716.
8. Perkel, D. J., Petrozzino, J. J., Nicoll, R. A. & Connor, J. A. (1993) *Neuron* **11,** 817–823.
9. Sorra, K. E. & Harris, K. M. (1993) *J. Neurosci.* **13,** 3736–3748.
10. Hessler, N. A., Shirke, A. M. & Malinow, R. (1993) *Nature (London)* **366,** 569–572.
11. Rosenmund, C., Clements, J. D. & Westbrook, G. L. (1993) *Science* **262,** 754–756.
12. Murphy, T. H., Baraban, J. M., Wier, W. G. & Blatter, L. A. (1994) *Science* **263,** 529–532.
13. Alger, B. E. & Nicoll, R. A. (1982) *J. Physiol. (London)* **328,** 105–123.
14. Lasser-Ross, N., Miyakawa, H., Lev-Ram, V., Young, S. R. & Ross, W. N. (1991) *J. Neurosci. Methods* **36,** 253–261.
15. Crunelli, V. & Mayer, M. L. (1984) *Brain Res.* **311,** 392–396.
16. Nowak, L., Bregestovski, P., Ascher, P., Herbet, A. & Prochiantz, A. (1984) *Nature (London)* **307,** 462–465.
17. Grynkiewicz, G., Poenie, M. & Tsien, R. Y. (1985) *J. Biol. Chem.* **260,** 3440–3450.
18. Neher, J. & Augustine, G. J. (1992) *J. Physiol. (London)* **450,** 273–301.
19. Johnston, D. & Brown, T. H. (1983) *J. Neurophysiol.* **50,** 464–486.
20. MacDermott, A. B., Mayer, M. L., Westbrook, G. L., Smith, S. J. & Barker, J. L. (1986) *Nature (London)* **321,** 519–522.
21. Regehr, W. G. & Tank, D. W. (1990) *Nature (London)* **345,** 807–810.
22. Schwarzkroin, P. A. (1975) *Brain Res.* **85,** 423–435.
23. Jaffe, D. B., Johnston, D., Lasser-Ross, N., Lisman, J. E., Myiakawa, H. & Ross, W. N. (1992) *Nature (London)* **357,** 244–246.
24. Lisman, J. E. & Harris, K. M. (1993) *Trends Neurosci.* **16,** 141–147.
25. Fox, S. E. & Rank, J. B. (1981) *Exp. Brain Res.* **249,** 315–331.
26. Buzsaki, G., Leung, L. S. & Vanderwolf, C. H. (1983) *Brain Res. Rev.* **6,** 139–171.